Nano World Journal

https://doi.org/10.17756/nwj.2017-045

Research Article

Open Access

Mimosa pudica Flower Extract Mediated Green Synthesis of Gold Nanoparticles

Krishnaprabha Mapala and Manjunatha Pattabi*

Department of Materials Science, Mangalore University, Mangalagangothri-574199, India

***Correspondence to:**
Manjunatha Pattabi, PhD
Department of Materials Science
Mangalore University
Mangalagangothri-574199, India
Tel: +91-824-2287249
E-mail: manjupattabi@yahoo.com

Received: March 24, 2017
Accepted: July 07, 2017
Published: July 11, 2017

Citation: Mapala K, Pattabi M. 2017. *Mimosa pudica* Flower Extract Mediated Green Synthesis of Gold Nanoparticles. *NanoWorld J* 3(2): 44-50.

Published by United Scientific Group

Abstract

The use of *Mimosa pudica* flower extract in the synthesis of highly stable gold nanoparticles (AuNPs) is reported here. On treatment of aqueous chloroauric acid with crude aqueous extract of *Mimosa pudica* flowers, rapid reduction of Au^{3+} ions at room temperature was observed without the need of any additional reducing or stabilizing agent. The synthesized AuNPs were characterized by UV–Vis spectroscopy, Field Emission Scanning Electron Microscopy (FESEM), Transmission Electron Microscopy (TEM), Dynamic Light Scattering (DLS) and Zeta potential, X-Ray Diffraction (XRD) and Fourier Transform Infra-Red (FTIR) spectroscopy. UV-Vis studies indicated the formation of AuNPs. The AuNPs were almost spherical in shape with an average particle size of 24 nm as determined by FESEM, TEM and DLS particle size analysis. XRD studies and high resolution TEM images ascertained the crystalline nature of the AuNPs. FTIR analysis of flower extract and AuNPs showed the possibility of phenolic group as responsible for the reduction of Au^{3+}. The stability of the AuNPs was analyzed by Zeta potential measurements. A negative Zeta potential value of -33.4 mV proved the stability of the AuNPs. The as synthesized AuNPs exhibited good catalytic activity in the model reduction reaction of 4-Nitrophenol to 4-Aminophenol.

Keywords

Mimosa pudica, AuNPs, Catalytic activity, FESEM, TEM

Introduction

Synthesis of gold nanoparticles (AuNPs) is an important field of nanotechnology as these particles find tremendous applications in arenas like cancer therapeutics [1], bioimaging [2, 3], optoelectronics [4], catalysis [5-7], biosensing [8] etc. In addition to the various physical and chemical synthesis routes, synthesis of noble metal nanoparticles using biological materials has emerged as a potential research area. The reducing and capping abilities of different biomaterials like bacteria, fungi and extracts prepared from various parts of the plants like leaf, stem, bark, peel, fruit, root are utilized to synthesize metal nanoparticles, thereby avoiding the usage of synthetic chemicals thus leading to benign, eco-friendly and cost-effective techniques [9-12]. AuNPs were synthesized by heating the mixture of gold precursor solution and extracts of flowers like *Nyctanthes arbortristis*, *Achillea wilhelmssi*, *Gnidea glauca* [13], *Lonicera japonica* [14] and *Allamanda* [15]. Room temperature synthesis of AuNP was reported by mixing the gold precursor solution and aqueous extract of flowers like *Rosa hybrida* [11], *Mirabilis jalapa* [13], *Rosa damascena* [15] and *Couroupita guianensis* [16]. Incubation of gold precursor solution and aqueous flower extract for few hours yielding AuNPs was reported using flowers like *Ixora*

Coccinia, *Caesalpenia pulcherrima (linn)* [17] and *Plumeria alba* linn [18]. AuNPs synthesized using plant extracts as reducing agent are used in applications like anticancer activities [16], antimicrobial activities [17, 18] and catalytic activities for the reduction reaction of 4-Nitrophenol [13] and H_2O_2 [15].

This paper reports the room temperature synthesis of stable AuNPs using *Mimosa pudica* flower extract as reducing agent. *Mimosa pudica* commonly known as touch-me-not or sensitive plant, is widely found as pantropical weed in tropical regions of India and other parts of the world. *Mimosa pudica* is a member of the family Fabaceae. Parts of *Mimosa pudica* plant (like roots, stem, leaves, flowers, and fruits) are used in traditional medicinal systems like Ayurveda and Unani to treat various ailments such as tooth ache, skin problems, bronchitis, gynaecological disorder, blood impurities, piles, jaundice etc. It is also used to treat neurological problems, diarrhoea, amoebic dysentery, blood arresting, urinary infections, wound healing etc. [19].

Several studies on *Mimosa pudica* have revealed the presence of phytochemicals such as tannins, flavonoids, triterpenes, steroids, alkaloids, carbohydrates, proteins, amino acids, phenolics, saponins, mucilage and glycosyl flavones [20]. Several research groups synthesized silver nanoparticles (AgNPs) using the leaf extract of *Mimosa pudica* as reducing agent [21-23]. Sreenivasulu et al. synthesized AgNPS using *Mimosa pudica* root extract [24]. Uma Suganya et al. synthesized AuNPs using leaf extract of *Mimosa pudica* and studied AuNP's anti-proliferative effect against breast cancer cell lines [25]. Iram et al. synthesized both AuNPs and AgNPs by reducing the gold and silver precursor solution with glucoxylan separated from the seeds of *Mimosa pudica* [26]. In the present study, flowers of *Mimosa pudica* were chosen to prepare the extract with the intention of carrying out simpler synthesis protocol involving less time and less cleaning steps. In fact, use of flower extract in the synthesis of AuNPs is less explored than the leaf extract mediated synthesis of AuNPs. Also, it is expected that AuNPs synthesized using the flower of *Mimosa pudica* might have medicinal properties as the plant has enumerable medicinal properties. This paper presents the potential of *Mimosa pudica* flower extract in the synthesis AuNPs at room temperature and the synthesized AuNPs were found to be stable and catalytically very active in the reduction reaction of 4-Nitrophenol.

Experimental Details

Materials and methods

$HAuCl_4 \cdot 3H_2O$ is procured from Central Drug House (CDH) and used as received as the source of Au^{3+}. Sodium borohydride ($NaBH_4$) and 4-Nitrophenol were obtained from Sigma-Aldrich and used without further purification. Deionized water is used for preparing all aqueous solutions.

Fresh flowers of *Mimosa pudica* were freshly collected, weighed and thoroughly washed with deionized water. Known amount of flowers (0.25 g/0.5 g/1 g) put in a beaker containing 25 mL deionized water was heated to boiling, continued heating for 2 more min after boiling and then allowed to cool before filtering. The filtrate was used for AuNP synthesis. Reaction mixture containing 4 mL of flower extract (any one of the 3 concentrations) and 16 mL of aqueous solution of chloroauric acid (0.25 mM) was continuously stirred at room temperature and observed for changes in color. The AuNP samples were named as MPAu-C1, MPAu-C2 and MPAu-C3 respectively for concentrations C1, C2 and C3. Similar experiments were carried out by adding different volumes (1-4 mL) of flower extract concentration C3 to $HAuCl_4$ solution (Samples MPAu-V1, MPAu-V2, MPAu-V3 and MPAu-V4) with final volume being 20 mL. Effect of temperature on the formation of AuNPs is checked by adding the flower extract of concentration C2 to the boiled gold precursor solution (MPAu-T).

The catalytic activity of the synthesized AuNPs is tested with the standard reduction reaction of 4-Nitrophenol to 4-Aminophenol by $NaBH_4$ 2 mL of AuNPs is added to stirred mixture of 1 mL of 4-Nitrophenol (5 mM) and 1 mL of $NaBH_4$ (0.25 M) in 25 mL of deionized water and the reduction reaction is monitored continuously as a function of time.

Characterization of the samples

The formation of AuNPs and the catalytic activity of synthesized AuNPs were monitored by recording the UV-Vis absorbance spectra for all the solutions using Shimadzu UV–1800 UV-Vis spectrophotometer operated at a resolution of 1 nm. Morphological characterization was carried out using a Carl Zeiss Field Emission Scanning Electron Microscope (FESEM) model Σigma operated at an accelerating voltage of 5 kV. Sample for FESEM analysis was prepared by placing a drop of the AuNP colloid on a piece of thin aluminium sheet. Transmission Electron Microscope (TEM) images of samples dried on carbon coated copper grid were obtained using JEOL 3010 TEM operated at 200 kV. Particle size range and surface charge of AuNPs were studied by dynamic light scattering (DLS) measurement and Zeta potential analysis using TRI Blue- Microtrac instrument. The Fourier Transform Infra-Red (FTIR) spectra of AuNP colloid and the flower extract were recorded using Shimadzu IR Prestige-21 FTIR spectrophotometer in order to identify the functional groups that are bound to the surface of nanoparticles and lead to the stability of nanoparticles.

Results and Discussion

A schematic illustration of AuNP synthesis is shown in Figure 1. The addition of *Mimosa pudica* flower extract to gold precursor solution initiates the reduction of Au^{3+} ions to Au° which is understood by the color changes of gold precursor solution from light yellow to shade of ruby red. The presence of ample phytochemicals in the flower extract act as both reducing and capping agent.

UV-Vis studies

The formation of AuNPs from chloroauric acid solution after the addition of flower extract is inferred both visually and by UV-Vis absorption spectra. Depending upon size,

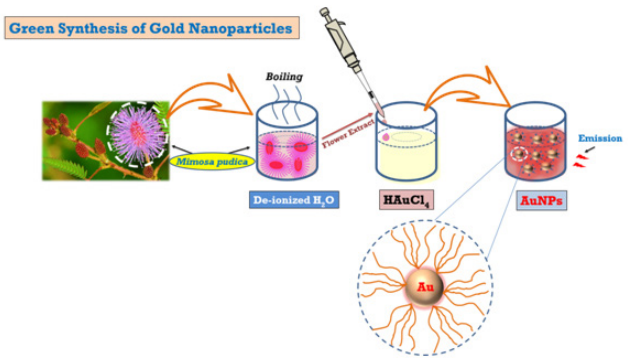

Figure 1: Schematic diagram representing the mechanism of formation of AuNPs.

shape and degree of aggregation, AuNPs exhibit different colors due to the collective oscillation of conduction band electrons on absorption of visible light, known as surface plasmon resonance (SPR) and thus, provide an easy way for visual detection of formation of AuNPs. The color transition of $HAuCl_4$ solution from pale yellow to a ruby red indicates the change in metal oxidation state and formation of AuNPs. Spherical AuNPs exhibit absorption peaks in visible region whereas the anisotropic particles give rise to absorption peaks both in visible and near infrared (NIR) region [27-29]. Figure 2A shows UV-Vis absorbance spectra of AuNPs synthesized at 100 °C and at room temperature. Synthesis at 100 °C involved faster reduction of Au^{3+} ions but the characteristic absorption band had no significant shift as seen in Figure 2A. However, the AuNPs synthesized at 100 °C are found to be stable even after 6 months which is not the case with AuNPs prepared at room temperature (2 months)

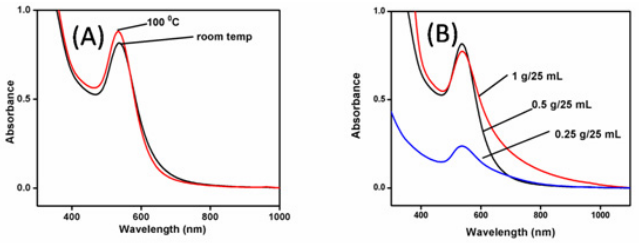

Figure 2: (A) UV-Vis absorbance spectra of AuNPs synthesized at different temperature (Mixture of 4 mL of flower extract with concentration C2 (0.5 g/25 mL) and 16 mL of 0.25 mM $HAuCl_4$ solution), **(B)** UV–Vis spectra of AuNPs synthesized by reacting 0.25 mM $HAuCl_4$ aqueous solution with varying concentrations of flower extract.

Figure 2B shows the UV-Vis absorption spectra of AuNP samples prepared at room temperature using varying concentrations of flower extract. The SPR peak is found to be at ~538 nm for all three concentrations of flower extract used. The reduction time of Au^{3+} ions was drastically reduced with the increase in the concentration of flower extract. Formation of more AuNPs at higher concentrations of flower extract is indicated by the increase in absorbance intensities of SPR bands. The formation of AuNPs with 0.25 g/25 mL of flower extract took more than 3 h whereas the formation was complete within 15 min with 0.5 g/25 mL. However, the optical studies reveal that polydispersity is more with AuNP colloid prepared with 1 g/25 mL flower extract, exhibiting a broader spectra.

AuNPs prepared by variation of volume of flower extract keeping total volume constant, did not show much change in SPR except for a very small shift in SPR peak with increasing volume of flower extract. Figure 3A represents the UV-Vis absorbance spectra of AuNP samples MPAu-V1 (1 mL) to MPAu- V4 (4 mL). Slight increase in intensity of absorption is observed with the increase in volume of flower extract. However, the SPR band of AuNP sample MPAu-V4 (with 4 mL flower extract) was broadened with decrease in intensity of absorption thus indicating an increase in polydispersity. A bulge in NIR region is observed with MPAu-V2 sample suggesting the presence of some anisotropic particles. Figure 3B represents the UV-Vis absorbance spectra of the same AuNP samples taken on day 5. AuNP sample MPAu-V1 (with 1 mL of flower extract) showed two fold increase in intensity of absorption and blue shift in SPR peak from 545 to 532 nm from day 1 to day 5. The remaining 3 samples did not show such changes thereby confirming the stability of AuNP samples.

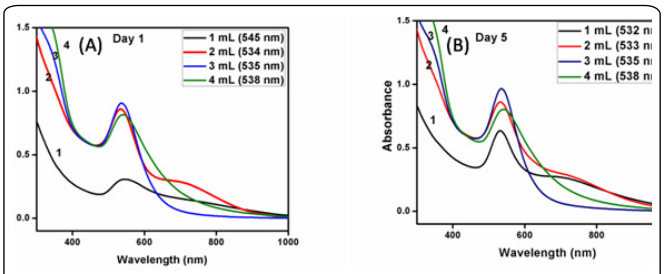

Figure 3: UV-Vis absorption spectra of AuNPs obtained by adding varying volumes of flower extract (1 g/25 mL) **(A)** on day 1 **(B)** on day 5.

Figure 4 shows the growth rate of AuNPs for the sample prepared by adding 4 mL of flower extract of concentration C3 (1 g/25 mL) to 16 mL of 0.25 mM $HAuCl_4$ solution at room temperature. The readings taken at 0.5 min soon after the addition of flower extract to gold precursor solution exhibit an absorption peak at 344 nm which is due to flower extract and vanishes after 1 min showing that the extract has started reducing the gold precursor. The steady increase in

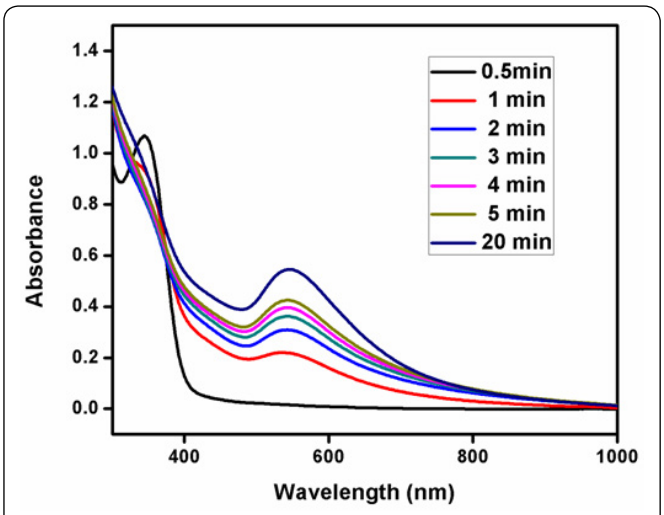

Figure 4: Onset and growth of AuNPs formed by adding 4 mL of flower extract of concentration C3 (1 g/25 mL) to 16 mL of 0.25 mM $HAuCl_4$ solution at room temperature.

intensity of absorption as a function of reaction time without any major shift in the SPR peak wavelength is seen as reported in literature [14].

FESEM studies

The surface morphology of the AuNPs is examined using FESEM. Figure 5A shows the FESEM micrograph of AuNP sample MPAu-2 along with its histogram depicting the size of AuNPs in Figure 5B. Well defined spherical AuNPs without any agglomeration are seen from the images. The particle size analysis is carried out with ImageJ software. Gaussian fitting is carried out to determine the average size of the AuNP and is found to be ~24 nm with a standard deviation of 5.42 nm.

Figure 6A represents the FESEM micrograph of AuNP

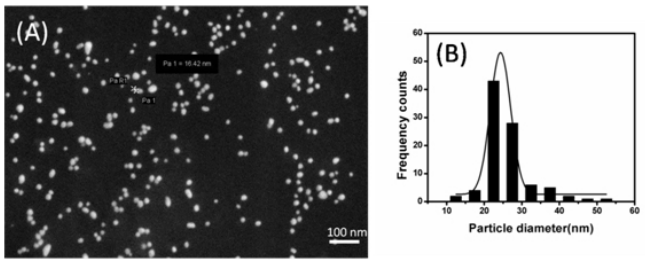

Figure 5: (A) FESEM micrograph of AuNP sample MPAu-C2, **(B)** Particle size distribution.

sample MPAu-V2. Presence of triangular and some disc shaped nanoparticles in addition to spherical nanoparticles confirm the anisotropy as depicted by UV measurements shown in Figure 3A and Figure 3B. Figure 6B represents the FESEM micrograph of AuNP sample MPAu-T synthesized at 100 °C. The micrograph shows the presence of some irregular shaped nanoparticles.

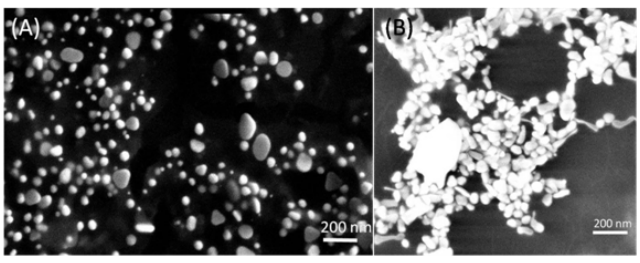

Figure 6: FESEM micrograph of **(A)** AuNP sample MPAu-V2, **(B)** AuNP sample (MPAu-T) prepared at 100 °C by adding 4 mL flower extract (0.5 g/25 mL) to 16 mL of 0.25 mM $HAuCl_4$.

TEM studies

Figure 7A shows the TEM micrograph of AuNP sample MPAu-C2 obtained at a magnification of 60000x and Figure 7B shows the HRTEM image of the same sample at a magnification of 800000x. Both the TEM and HRTEM micrographs clearly elucidate the size, shape, and morphology of synthesized AuNPs. The HRTEM image displayed clear lattice fringes on the nanoparticle surface.

DLS studies

Figure 8 shows the size distribution of AuNPs determined by the Zeta study and the average hydrodynamic size of AuNPs is found to be ~24 nm. The surface charge of AuNP was found to be -33.4 mV. High negative value of the Zeta potential is indicative of high electrical charge on the surface of the AuNPs due to which strong repulsion between AuNPs, thereby, avoiding aggregation and suggesting higher stability of the AuNP colloid [30]. The negative potential value might be due to the capping action of biomolecules present in the flower extract of *Mimosa pudica*.

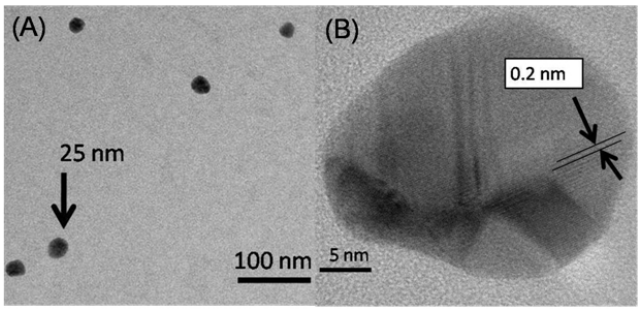

Figure 7: (A) TEM micrograph of MPAu-C2, **(B)** HRTEM micrograph of MPAu-C2.

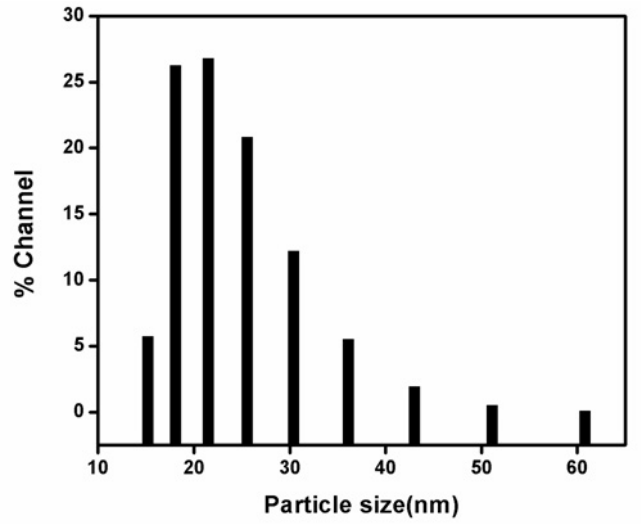

Figure 8: Particle size distribution by DLS of AuNP sample MPAu-C2, showing mean diameter of ~24 nm.

XRD studies

Figure 9 shows the XRD pattern of the sample MPAu-C2. Formation of pure crystalline AuNPs is confirmed by Bragg's reflection at 2θ = 37.91° which is ascribed to (111) facets of face centered cubic nature of AuNPs (JCPDS file no. 04-0784). Enlarged pattern of (111) peak along with Gaussian fitting is shown in the inset of XRD graph using which full width half maximum (FWHM) is determined. The average size of the AuNPs was found to be about 12 nm as calculated by Scherrer equation

$$S = \frac{k.\lambda}{\beta.\cos\theta}$$

where S is the crystallite size of AuNPs, λ is the wavelength of the X-ray source (1.54056 Å) used in the XRD, β is the FWHM of the (111) diffraction peak in radian, k is the Scherrer constant that varies from 0.9 to 1 (taken 0.9) and θ is the Bragg angle in radian [31].

The interplanar spacing and lattice parameter for (111) plane was found to be 0.236 nm and 0.409 nm respectively. The calculated values agree with the standard lattice parameter of 0.40729 nm for metallic gold.

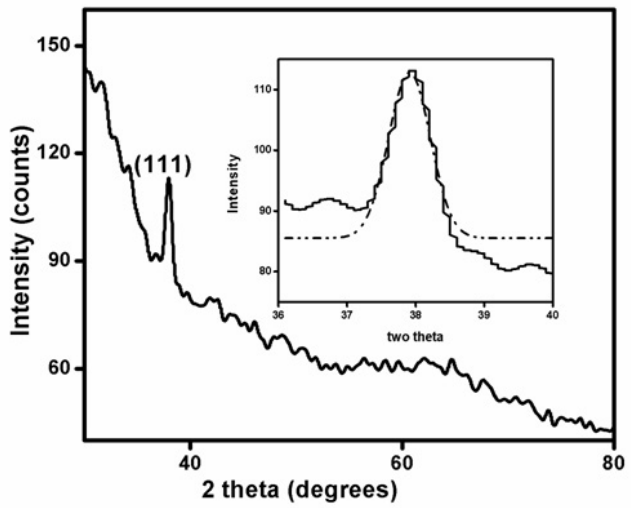

Figure 9: XRD pattern of AuNP sample MPAu-C2.

FTIR studies

FTIR spectrum of flower extract and one of the AuNP samples are shown in Figure 10. Peaks centered at the 3294 cm^{-1} is found in the FTIR spectrum of flower extract. The intense absorption peak located at 3294 cm^{-1}, can be attributed to the -OH stretching modes of vibration in alcohols which got shifted to 3331 cm^{-1} for the AuNP sample and flower extract, thereby indicating that –OH group is mainly responsible for the reduction of Au^{3+} to Au. The small change in amplitude of peak and a shift from 3294 to 3331 cm^{-1} observed with the values found in case of AuNP colloid may be attributed to the capping of the species as reported in literature [32].

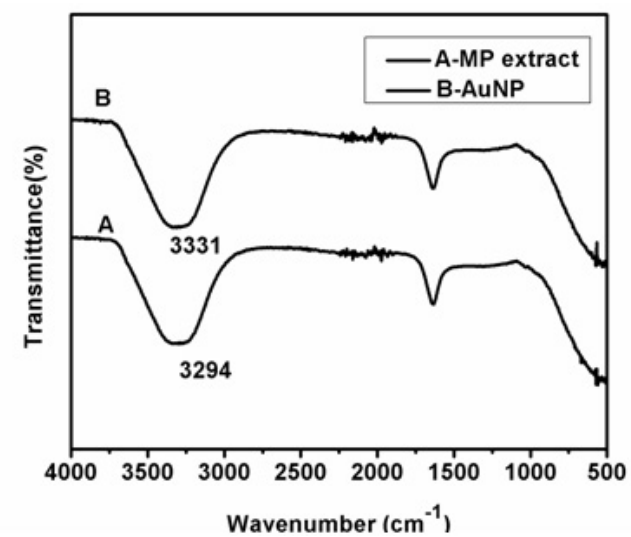

Figure 10: FTIR spectra of flower extract and AuNPs synthesized using 4 mL of 0.5 g/25 mL of flower extract.

Catalytic activity

It is reported that in the absence of catalyst, aromatic nitro compounds are inert to the reduction by $NaBH_4$ [33]. An aqueous solution of 4-Nitrophenol exhibits two absorption peaks at 226 and 317 nm corresponding to *π→π (from the ring of phenol) and *π→n (from lone pair of electron in the oxygen and nitrogen atom) represented by curve 1 in Figure 11A [34]. After the addition of $NaBH_4$, color change from light yellow to yellowish green confirmed by UV-Vis spectra shows a shift in absorption peak from 317 to 400 nm which is due to the generation of 4-nitrophenolate anions in the reaction system as reported in literature [7, 13, 35]. The SPR peak at 400 nm remains unaltered for couple of days in the absence of AuNPs as reported in literature [33, 36]. The catalyst helps this reduction process by conveying electrons from the donor BH_4^- ions to the acceptor 4-nitrophenolate ions both of which are adsorbed on the catalyst surface. After the addition of 2 mL of AuNPs, the hypochromic change in the intensity of absorption of nitrophenolate ions was monitored by recording the readings with UV-Vis spectrophotometer. The visual inspection of the solution showed gradual color fading which is due to the consumption of 4-Nitrophenol. While the intensity at 400 nm decreased, emergence of the new peak at 300 nm, which gradually increased in its intensity, suggested the formation of 4-Aminophenol as shown in Figure 11A.

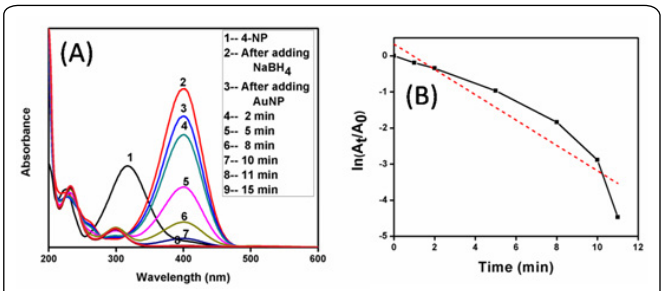

Figure 11: (A) Time dependent UV–Vis spectra for monitoring 4-Nitrophenol reduction by $NaBH_4$ catalyzed by AuNPs sample MPAu-C2, **(B)** Plot of ln (At/Ao) with time at 400 nm for 4-Nitrophenol reduction by $NaBH_4$ in presence of AuNP (MPAu-C2).

As the concentration of $NaBH_4$ used was much higher than that of 4-Nitrophenol, the order of the reaction was considered to be pseudo-first order reaction [37-39]. Therefore, the catalytic rate constant (K) in this case is evaluated by studying the pseudo-first-order kinetics with respect to 4-Nitrophenol concentration. The ratio of absorbance A_t of 4-Nitrophenol at time 't' to its value A_0 measured at t = 0 must be equal to the concentration ratio (C_t/C_0) of 4-Nitrophenol, the kinetic equation for the reduction can be expressed as

$$\frac{dC_t}{dt} = -kC_t \text{ or } \ln\left(\frac{c_t}{c_o}\right) = \ln\left(\frac{A_t}{A_0}\right) = -Kt$$

where C_t is the concentration of 4-Nitrophenol at time t and k is the apparent rate constant, which can be obtained from the decrease of the peak intensity at 400 nm with time. The graph in Figure 11B shows good linear correlation of $\ln\left(\frac{A_t}{A_0}\right)$ versus time and the kinetic rate reaction constant was estimated to be 0.3 min^{-1}.

Conclusions

AuNPs are synthesized by reducing gold precursor solution with *Mimosa pudica* flower extract at room temperature. The synthesis method can be considered as non-polluting, energy efficient as the synthesis procedure does not require stirring, heating and even change of pH. The size of AuNPs determined by FESEM, TEM and DLS studies are consistent with one another. Excellent catalytic activity was observed during the reduction of 4-Nitrophenol. The synthesized AuNPs were stable and were well capped which are very important from the aspects of its bio-medical application such as contrasting agents in bio-imaging.

Acknowledgement

One of the authors, (KM) thanks the University Grants Commission for the financial assistance through FIP scheme. Thanks are also due to DST- PURSE facility for UV-Vis readings and FESEM images.

References

1. Jain S, Hirst DG, O'Sullivan JM. 2012. Gold nanoparticles as novel agents for cancer therapy. *Br J Radiol* 85(1010): 101-113. https://doi.org/10.1259/bjr/59448833
2. Schultz DA. 2003. Plasmon resonant particles for biological detection. *Curr Opin Biotechno* 14(1): 13-22. https://doi.org/10.1016/S0958-1669(02)00015-0
3. Salem AK, Searson PC, Leong KW. 2003. Multifunctional nanorods for gene delivery. *Nature Mater* 2: 668-671. https://doi.org/10.1038/nmat974
4. Hu M-S, Chen H-L, Shen CH, Hong L-S, Huang B-R, et al. 2006. Photosensitive gold nanoparticles embedded dielectric nanowires. *Nature Mater* 5: 102-106. https://doi.org/10.1038/nmat1564
5. Hvolback B, Janssens TVW, Clausen BS, Falsig H, Christensen CH, et al. 2007. Catalytic activity of Au nanoparticles. *Nanotoday* 2(4): 14-18. https://doi.org/10.1016/S1748-0132(07)70113-5
6. Narayanan R, El-Sayed MA. 2005. Catalysis with transition metal nanoparticles in colloidal solution: nanoparticle shape dependence and stability. *J Phys Chem B* 109(26): 12663-12676. https://doi.org/10.1021/jp051066p
7. Rashid MH, Bhattacharjee RR, Kotal A, Mandal TK. 2006. Synthesis of spongy gold nanocrystals with pronounced catalytic activities. *Langmuir* 22(17): 7141-7143. https://doi.org/10.1021/la060939j
8. Li Y, Schluesener HJ, Xu S. 2010. Gold nanoparticles-based biosensors. *Gold Bulletin* 43(1): 29-41. https://doi.org/10.1007/BF03214964
9. Narayanan KB, Sakthivel N. 2011. Green synthesis of biogenic metal nanoparticles by terrestrial and aquatic phototrophic and heterotrophic eukaryotes and biocompatible agents. *Adv Colloid Interface Sci* 169(2): 59-79. https://doi.org/10.1016/j.cis.2011.08.004
10. Mittal AK, Chisti Y, Banerjee UC. 2013. Synthesis of metallic nanoparticles using plant extracts. *Biotechnol Adv* 31(2): 346-356. https://doi.org/10.1016/j.biotechadv.2013.01.003
11. Kavitha KS, Baker S, Rakshith D, Kavitha HU, Rao HCY, et al. 2013. Plants as green source towards synthesis of nanoparticles. *Int Res J Biological Sci* 2(6): 66-76.
12. Varahalarao V, Kaladhar DSVGK. 2014. Review: Green synthesis of silver and gold nanoparticles. *Middle-East J Sci Res* 19(6): 834-842.
13. Ghosh S, Patil S, Ahire M, Kitture R, Gurav DD, et al. 2012. *Gnidia glauca* flower extract mediated synthesis of gold nanoparticles and evaluation of its chemocatalytic potential. *J Nanobiotechnology* 10: 17. https://doi.org/10.1186/1477-3155-10-17
14. Nagajyothi PC, Lee SE, An M, Lee KD. 2012. Green synthesis of silver and gold nanoparticles using *Lonicera japonica* flower extract. *Bull Korean Chem Soc* 33(8): 2609- 2612. https://doi.org/10.5012/bkcs.2012.33.8.2609
15. Gangwar RK, Dhumale VA, Gosavi SW, Sharma RB, Datar SS. 2013. Catalytic activity of allamanda mediated phytosynthesized anisotropic gold nanoparticles. *Adv Nat Sci: Nanosci Nanotechnol* 4: 045005. https://doi.org/10.1088/2043-6262/4/4/045005
16. Geetha R, Ashok KT, Tamilselvan S, Govindaraju K, Sadiq M, et al. 2013. Green synthesis of gold nanoparticles and their anticancer activity. *Cancer Nano* 4(4-5): 91-98. https://doi.org/10.1007/s12645-013-0040-9
17. Nagaraj B, Divya TK, Malakar B, Krishnamurthy NB, Dinesh R, et al. 2012. Phytosynthesis of gold nanoparticles using *Caesalpinia pulcherrima* (peacock flower) flower extract and evaluation of their antimicrobial activities. *Dig J Nanomater Biostruct* 7(3): 899 - 905.
18. Nagaraj B, Malakar B, Divya TK, Krishnamurthy NB, Liny P, et al. 2012. Environmental benign synthesis of gold nanoparticles from the flower extracts of *Plumeria alba* Linn. (Frangipani) and evaluation of their biological activities. *Int J Drug Dev & Res* 4(1): 144-150.
19. Varnika S, Ashish S, Imran A. 2012. A review of ethnomedical and traditional uses of *Mimosa pudica* (Chui-Mui). *IJRP* 3(2): 41-44.
20. Muhammad G, Hussain MA, Jantan I, Bukhari SNA. 2016. *Mimosa pudica* L., a High-value medicinal plant as a source of bioactives for pharmaceuticals. *Comprehensive Reviews in Food Science and Food Safety* 15(2): 303-315. https://doi.org/10.1111/1541-4337.12184
21. Ganaie SU, Abbasi T, Abbasi SA. 2015. Green synthesis of silver nanoparticles using an otherwise worthless weed Mimosa (*Mimosa pudica*): feasibility and process development toward shape/size control. *Particulate Science and Technology* 33(6): 638-644. https://doi.org/10.1080/02726351.2015.1016644
22. Akash Raj S, Divya S, Sindhu S, Kasinthan K, Armugam P. 2014. Studies on synthesis, characterization and application of silver nanoparticles using *Mimosa pudica* leaves. *Int J Pharm Pharm Sci* 6(2): 453-455.
23. Afisa N, Mutiara L. 2016. Biosynthesis of silver nanoparticles using putri malu (*Mimosa pudica*) leaves extract and microwave irradiation method. *Molekul* 11(2): 288-298. https://doi.org/10.20884/1.jm.2016.11.2.221
24. Sreenivasulu V, Kumar NS, Suguna M, Asif M, Al-Ghurabi EH, et al. 2016. Biosynthesis of silver nanoparticles using *Mimosa pudica* plant root extract: characterization, antibacterial activity and electrochemical detection of dopamine. *Int J Electrochem Sci* 11(2016): 9951-9979. https://doi.org/10.20964/2016.12.69
25. Uma Suganyaa KS, Govindaraju K, Ganesh Kumar V, Prabhu D, Arulvasub C, et al. 2016. Anti-proliferative effect of biogenic gold nanoparticles against breast cancer cell lines (MDA-MB-231 & MCF-7). *Appl Surf Sci* 371: 415-424.
26. Iram F, Iqbal MS, Athar MM, Saeed MZ, Yasmeen A, et al. 2014. Glucoxylan-mediated green synthesis of gold and silver nanoparticles and their phyto-toxicity study. *Carbohydr Polym* 104: 29-33. https://doi.org/10.1016/j.carbpol.2014.01.002
27. Shankar SS, Rai A, Ahmad A, Sastry M. 2005. Controlling the optical properties of lemongrass extract synthesized gold nanotriangles and potential application in infrared-absorbing optical coatings. *Chem Mater* 17(3): 566-572. https://doi.org/10.1021/cm048292g
28. Ankamwar B, Chaudhary M, Sastry M. 2005. Gold nanotriangles biologically synthesized using tamarind leaf extract and potential application in vapor sensing. *Synth React Inorg M* 35: 19-26. https://doi.org/10.1081/SIM-200047527
29. Nikoobakht B, Wang J, El-Sayed MA. 2002. Surface-enhanced raman scattering of molecules adsorbed on gold nanorods: off-surface plasmon resonance conditions. *Chem Phys Lett* 366(1-2): 17-23. https://doi.org/10.1016/S0009-2614(02)01492-6
30. Dash SS, Bag BG, Hota P. 2015. *Lantana camara* Linn leaf extract mediated green synthesis of gold nanoparticles and study of its catalytic

activity. *Appl Nanosci* 5(3): 343-350. https://doi.org/10.1007/s13204-014-0323-4

31. Shankar SS, Ahmad A, Parischa R, Sastry M. 2003. Bioreduction of chloroaurate ions by geranium leaves and its endophytic fungus yields gold nanoparticles of different shapes. *J Mater Chem* 13(7): 1822-1826.
32. Philip D. 2009. Biosynthesis of Au, Ag and Au-Ag nanoparticles using edible mushroom extract. *Spectrochim Acta A Mol Biomol Spectrosc* 73(2): 374-381. https://doi.org/10.1016/j.saa.2009.02.037
33. Pradhan N, Pal A, Pal T. 2002. Silver nanoparticles catalyzed reduction of aromatic nitro compounds. *Colloids Surf A Physicochem Eng Asp* 196(2-3): 247-257. https://doi.org/10.1016/S0927-7757(01)01040-8
34. Seoudi R, Said DA. 2011. Studies on the Effect of the capping materials on the spherical gold nanoparticles catalytic activity. *World Journal of Nano Science and Engineering* 1(2): 51-61. https://doi.org/10.4236/wjnse.2011.12008
35. Saha S, Pal A, Kundu S, Basu S, Pal T. 2010. Photochemical green synthesis of calcium-alginate-stabilized Ag and Au nanoparticles and their catalytic application to 4-nitrophenol reduction. *Langmuir* 26(4): 2885-2893. https://doi.org/10.1021/la902950x
36. Hayakawa K, Yoshimura T, Esumi K. 2003. Preparation of gold-dendrimer nanocomposites by laser irradiation and their catalytic reduction of 4-nitrophenol. *Langmuir* 19(13): 5517-5521. https://doi.org/10.1021/la0343391
37. Gangula A, Podila R, Ramakrishna M, Karnam L, Janardhana C, et al. 2011. Catalytic reduction of 4-Nitrophenol using biogenic gold and silver nanoparticles derived from *Breynia rhamnoides*. *Langmuir* 27(24): 15268-15274. https://doi.org/10.1021/la2034559
38. Panigrahi S, Basu S, Praharaj S, Pande S, Jain S, et al. 2007. Synthesis and size selective catalysis by supported gold nanoparticles: study on heterogeneous and homogeneous catalytic process. *J Phys Chem C* 111(12): 4596-4605. https://doi.org/10.1021/jp067554u
39. Zhang J, Chen G, Chaker M, Rosei F, Ma D. 2013. Gold nanoparticle decorated ceria nanotubes with significantly high catalytic activity for the reduction of nitrophenol and mechanism study. *Appl Catal B* 132-133: 107-115. https://doi.org/10.1016/j.apcatb.2012.11.030